Arch. Metall. Mater. **67** (2022), 1, 357-370

DOI: https://doi.org/10.24425/amm.2022.137766

R. PALANIVEL[1*], S. VIGNESHWARAN[2], A. ALSHQIRATE[3],
R. MADHAVAN[2], P. VENKATACHALAM[4], R.F. LAUBSCHER[5]

EFFECT OF MACHINING PROCESS PARAMETERS AND NUMBER OF PASS ON COMPACTION BEHAVIOUR OF COMMERCIALLY PURE ALUMINIUM CHIPS CONSOLIDATED BY EQUAL CHANNEL ANGULAR PRESSING (ECAP) USING RESPONSE SURFACE METHODOLOGY

This work investigates the compaction behaviour of commercial pure aluminium chips (CP Al) produced during a machining operation and subsequently consolidated by Equal Channel Angular Pressing (ECAP). Empirical models were developed to describe the relative density and hardness of the compacted product of ECAP as functions of the initial machining input parameters including cutting edge angle (CA), depth of cut (DOC) and then the number of consolidation pass during ECAP. The models were developed utilizing response surface methodology (RSM) based on data from a central composite face centred factorial design of experiments approach. The models were then validated by using Analysis of Variance (ANOVA). The effect of input parameters on the relative density and hardness of the ECAP consolidated samples are presented and discussed including details as regards to the mechanical and microstructural properties. An optimum set of input parameters are identified and presented where the best relative density and hardness are demonstrated.

Keywords: ECAP; Response surface methodology; Relative density; Machining; Hardness; Chip consolidation

1. Introduction

Recycling of non-ferrous metal scraps reduces the extraction of new ores and prevents the environmental impacts, including emission of hazardous gases, disposal of solid wastes and destruction of earth surface [1]. Besides, recycling of non-ferrous metal scraps can conserve the energy however, care should also be taken while recycling scrap metals [2]. The major two classification of recycling non ferrous metal scraps, include, re-melting and solid-state recycling (without melting). As far as re-melting is concerned, melt loss, chemical reactivity, liberation of toxic gases, energy consumption and recycling costs are the overall challenges associated with it when compared to the solid-state recycling of metallic scraps. Solid-state recycling of metallic scraps is considered to be prolific particularly for machined chips as it can transform the chips into semi-finished or bulk metallic products with excellent mechanical properties [3].

Application of severe plastic deformation (SPD) methods have been developed and evaluated successfully for the solid-state recycling of metal scraps. SPD methods like, equal channel angular pressing (ECAP) [4], high pressure torsion (HPT) [5], friction stir extrusion (FSE) [6], cyclic extrusion and compression (CEC) [7] etc., are viable metal forming routes followed not only for producing ultra-fine-grained high strength materials but also not limited to produce solid bulk products form waste metal scraps.

Among the SPDs, the ECAP is a proven technique to impart significant plastic strain in pure bulk metals, alloys, composites and is typically also be used to refine grain sizes to ultra-fine levels [8,9]. ECAP was used to consolidate aluminium (Al) – Yttria composite powder by incorporating a back pressure. This produced a nearly fully relative density compaction at atmospheric temperature [4]. Back pressure assisted ECAP of Al particles produces bulk material with better metallurgical bonding when compared to the ECAP carried out with out the aid of back pressure [10]. Metallic materials, which are difficult to consolidate are improved by incorporating back pressure or increasing the processing temperature [11,12]. Haghighi

[1] SHAQRA UNIVERSITY, DEPARTMENT OF MECHANICAL ENGINEERING, SAUDI ARABIA, 11911
[2] NATIONAL INSTITUTE OF TECHNOLOGY, DEPARTMENT OF MECHANICAL ENGINEERING, PUDUCHERRY, KARAIKAL – 609 609, INDIA
[3] DEPARTMENT OF MECHANICAL ENGINEERING, FACULTY OF ENGINEERING TECHNOLOGY, AL-BALQA APPLIED UNIVERSITY, JORDAN 19117
[4] DEPARTMENT OF MECHANICAL ENGINEERING, MVJ COLLEGE OF ENGINEERING, BENGALURU – 560 067, KARNATAKA, INDIA
[5] DEPARTMENT OF MECHANICAL SCIENCE & ENGINEERING, UNIVERSITY OF JOHANNESBURG, SOUTH AFRICA

* Corresponding author: rpalanivelme@gmail.com

et al. [13] showed that the porosity of Al-5% Al_2O_3 composites are gradually reduced by increasing the number of ECAP passes. AZ91 Mg alloy machined chips were consolidation by ECAP. The consolidated AZ91 Mg chips produced high strength product when compared to a solid extruded ECAP sample. This is due to a more refined grain size and dispersion of the oxide contaminants when compared to the solid state recycle process [14]. Zhilyaev et al. [15] used high-pressure torsion for the cold-consolidation of copper chips produced by machining. Moreover, by using the machined chips of pure titanium a completely dense bulk product with fine grained structure with a combination of high strength and ductility has been developed by ECAP [16].

Aluminium and its alloys are important materials in the automotive, aviation and construction sectors due to their reduced density and adequate strength [17,18]. Limited literature is available as regards to chip consolidation of aluminium by ECAP [3,19]. The effects of the cutting parameters to produce the chips are even less well described. Cutting parameters that have a marked effect on the size and thickness of the chip include the depth of cut (DOC) and the cutting edge angle (CA), also referred to as the lead angle. These parameters along with the number of consolidation passes may have a significant effect on the relative density and hardness of the consolidated sample [20]. The quality of the consolidated metal chips depends on chip characteristics, die profile, and process parameters as it influences the quality of bonding and microstructure of the consolidated product [3]. In this study, a right-angled channel (f) ECAP die with a corner angle (y) of 20° was used to obtain the maximum shear stress to make the consolidation better. Though, changes in die profile has significant effect on consolidation behaviour, it involves additional cost. However, studying the characteristics of chips on the consolidation behaviour is lagging. This study aims to know about the significance of turned chips based on the CA, DOC in one hand and on the other hand the number of passes (ECAP process parameter) is also chosen. Using the aforementioned parameters, the present study deals with the understanding of the consolidation behaviour and bonding quality of the chips and so as the evolved microstructure of the consolidated product. The optimization is conducted by Response Surface Methodology (RSM), an integral statistical and mathematical tool for modelling and analysing of engineering problems.

The RSM is the mathematical and statistical techniques based on applying a polynomial formula to experimental knowledge, which must explain the behaviour of an information set to make statistical predictions, enhance and optimize the empirical model building parameter, and also to recognize the interaction of different factors that affect it. Numerous researchers [21-26] have used RSM in various engineering fields to predict the parameters for best response. Chari et al. [21] developed RSM based model to study the effect of equal-channel angular rolling parameters on the equivalent plastic strain. They reported that RSM provides artless relationships for the prediction of responses. Saleh et al. [22] studied the effect of wear testing parameters on the weight loss of the AZ91 magnesium alloy, which was generated by the different number of passes through the rotary die-equal channel angular pressing process. Shahraki et al. [23] used RSM to correlate relationship between factors and responses for spiral equal-channel extrusion of AA7075. Yang et al. [24] made an optimization for ECAP process to develop semisolid billet of AA 6061 using RSM. They reported that the errors between the experimental values and the predicted values of the response surface models are small enough, which verifies the reliability of the model. Velmanirajan et al. [25] utilised RSM to report optimal tensile properties of Al sheet based on sheet thickness, annealing temperature and specimen orientation as input variables. They also investigated the strain formability limit based on blank width, annealing temperature and sheet thickness as input parameters in the same study. Vettivel et al. [26] utilized RSM to predict the frictional coefficient and wear rate of nanocomposite powders subject to input parameters including sintering temperature, percentage weight of powders, load and distance of sliding**.** Hence this investigation presents the effect of selected process parameters (CA, DOC and number of passes) on the relative density and hardness of consolidated aluminium chips by ECAP. Optimal process parameters are obtained via RSM.

2. The experimental work was carried out as follows

2.1. Materials

The commercially pure (CP) Al with the chemistry (in wt.%) of 97.7% Al, 0.7 Mg, 0.58 Si, 0.53 Mn, 0.38 Fe and few traces of Zn, Cr, Sn and Ti was chosen as the investigated material.

2.2. Machining & ECAP process

The chips were turned from the CP Al rod using a positive rake angled (+12°) tungsten carbide tool as shown in Fig. 1. The turning operation was carried out on a light duty engine lathe with a spindle speed of 200 rpm. The cutting speed was kept

Fig. 1. (a) Turned CP Al chips

minimal to restrict the temperature rise in the chip formation zone. Besides, the diluted soluble oil was used as coolant for the entire turning operation. The chips were turned with three cutting edge angles (CA) namely, 60°, 75° and 90° and the depth of cut (DOC) was kept as 0.4 mm, 0.6 mm and 0.8 mm, respectively. The chips were stored in the desiccator to minimalize the interaction of chips with the atmosphere. The surface morphology of the collected chips was observed for any contamination and oxide layer formation through Vega 3 Tescan^{TM} scanning electron microscopy (SEM). The surface morphology of chips after the machining operation is shown in Fig. 2-4 for the various CAs and DOCs. The turned continuous chips were fragmented by

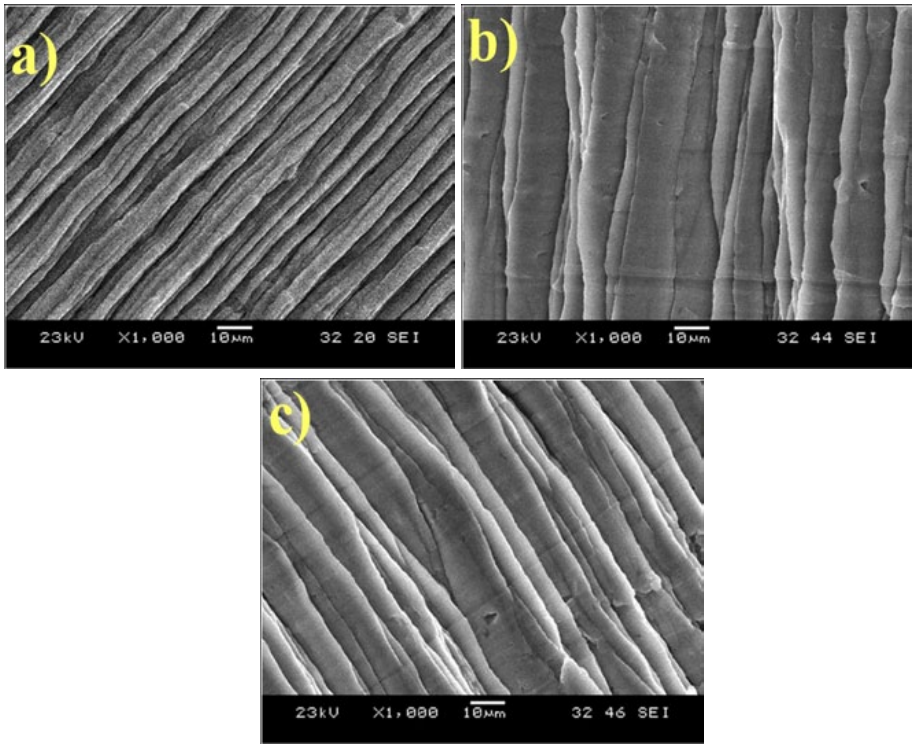

Fig. 2. Chip surface morphology for 0.4 mm DOC for: (a) 60°CA, (b) 75°CA and (c) 90°CA

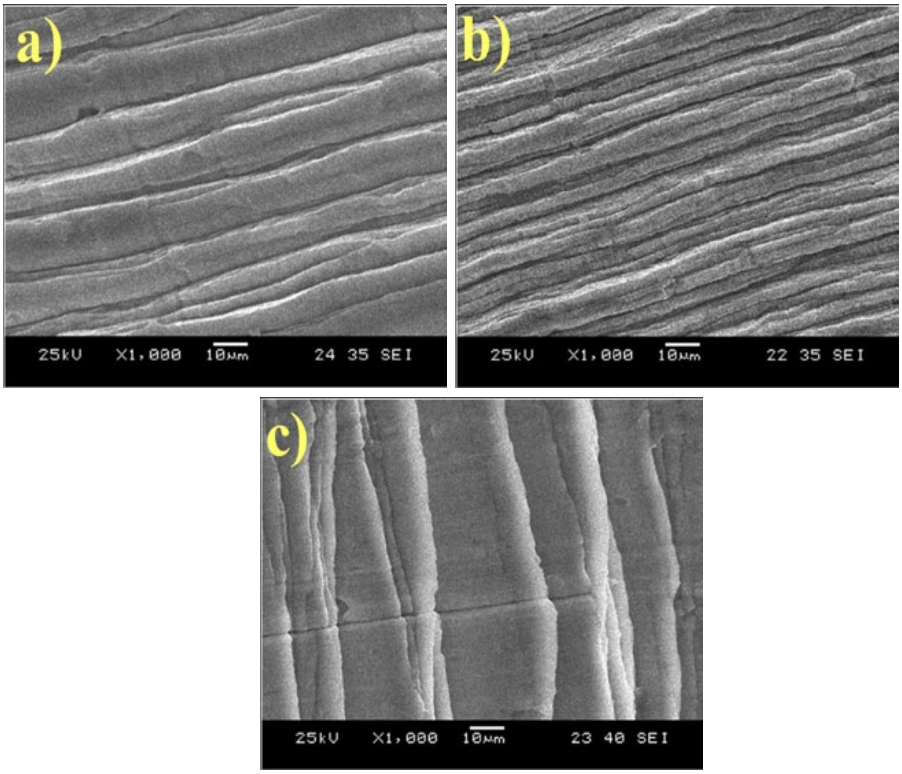

Fig. 3. Chip surface morphology for 0.6 mm DOC for: (a) 60°CA, (b) 75°CA and (c) 90°CA

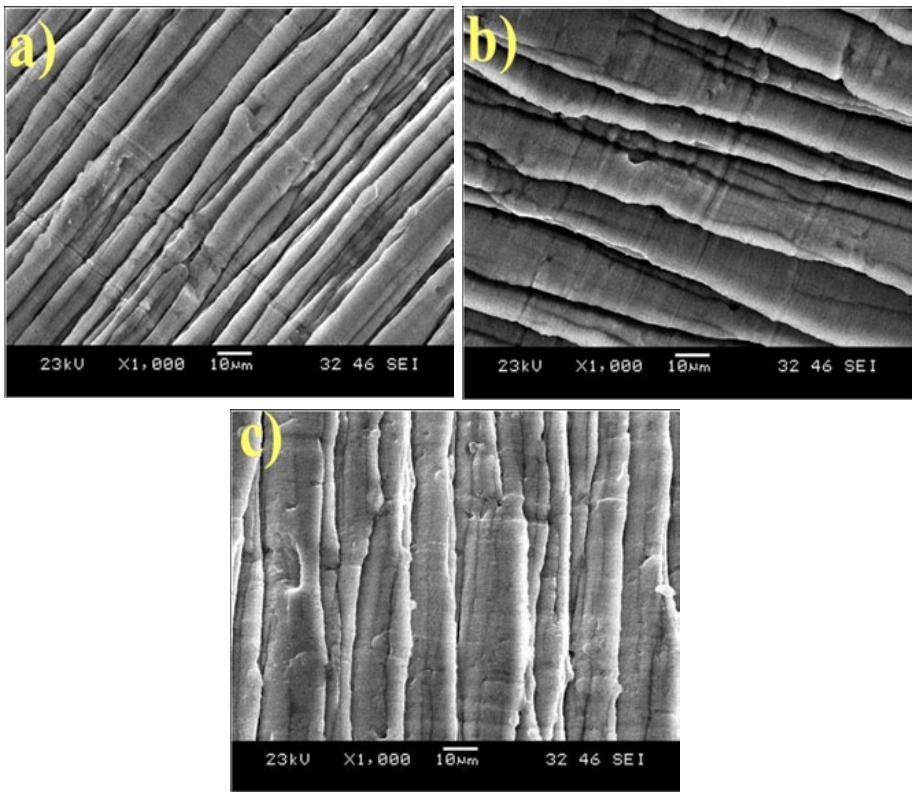

Fig. 4. Chip surface morphology for 0.8 mm DOC for: (a) 60°CA, (b) 75°CA and (c) 90°CA

hand, cleansed using toluene and then packed in the aluminium cans before the ECAP process. The surface morphology of the chip before encapsulating inside the Al can is shown in Fig. 5. The fabricated aluminium can and the back-pressure system are shown in Fig. 6a. Moreover, the full ECAP die setup is shown in Fig. 6b. The ECAP process was done with the aid of back pressure using a 589 MN capacity Universal Testing Machine (UTM) manufactured by Fuel Instruments and Engineers ™ as shown in Fig. 6c. A right-angled channel (f) ECAP die with a corner angle (y) of 20° followed by "route A" methodology was utilized for the chip consolidation. The MoS_2 (molybdenum disulphide) was used as lubricant for the side walls of ECAP die and approximately 98 MN of load was applied for chip compaction with a ram speed of 1 mm/s. The extruded samples of the different chosen parameter sets are shown in Fig. 7-9. The actual dimension of the extruded sample after 1st pass was around 50 mm in length and whereas, the final pass sample showed an overall length of nearly 25-30 mm. The relative density of the extruded samples was obtained by utilizing the Archimedes principle. Vickers micro hardness (HV) testing was conducted with a load of 2.94 N for 15 seconds at 5 different places on the cross plane of ECAP extruded sample and the average of the 5 readings is presented in Table 2. The consolidation behaviour of the chips with respect to various CA, DOC and number of passes, were observed using a light optical microscopy (Olympus™) on the cross plane of the extruded sample. For the optical microscopic observations, standard metallographic polishing method was adopted followed by 20s of etching using a Keller's reagent (2.5 ml of HNO_3, 1.5 ml of HCl, 1 ml of HF and 95 ml of distilled water). Furthermore, the etched surface was observed using a light optical microscope (Olympus™ BX51M) and using a SEM unit.

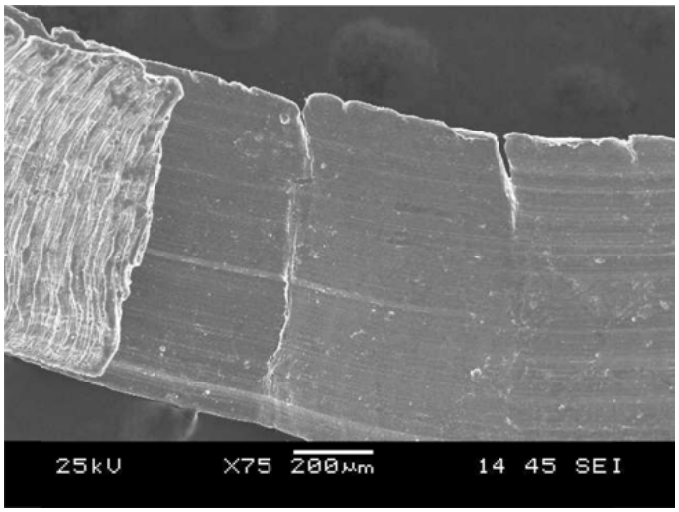

Fig. 5. Surface morphology of turned CP Al chip recorded before encapsulating inside the Al can

3. Response surface methodology (RSM) program

3.1. Input parameter selection

The input parameters selected for the current investigation is the CA, the DOC and the number of consolidation passes.

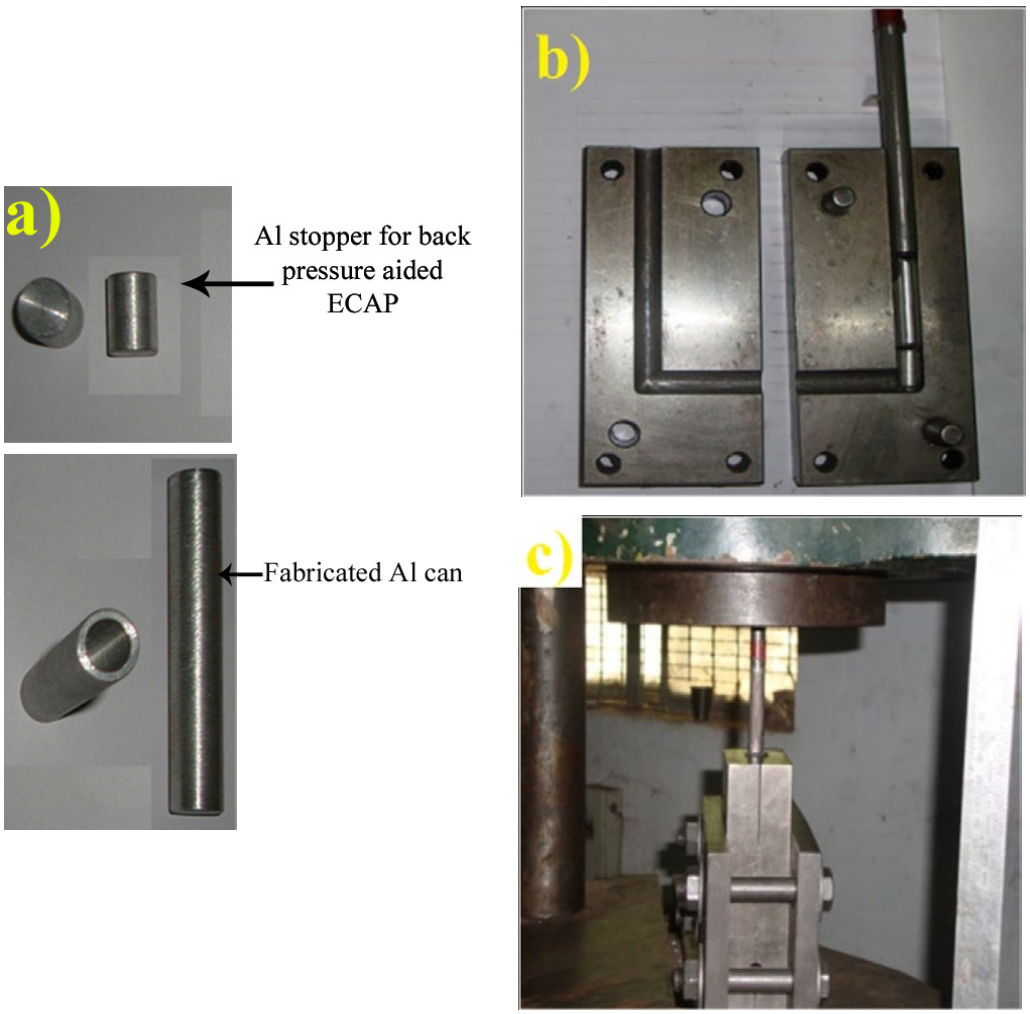

Fig. 6. (a) Fabricated Al can and back pressure system, (b) ECAP die setup, (c) ECAP die loaded under universal testing machine

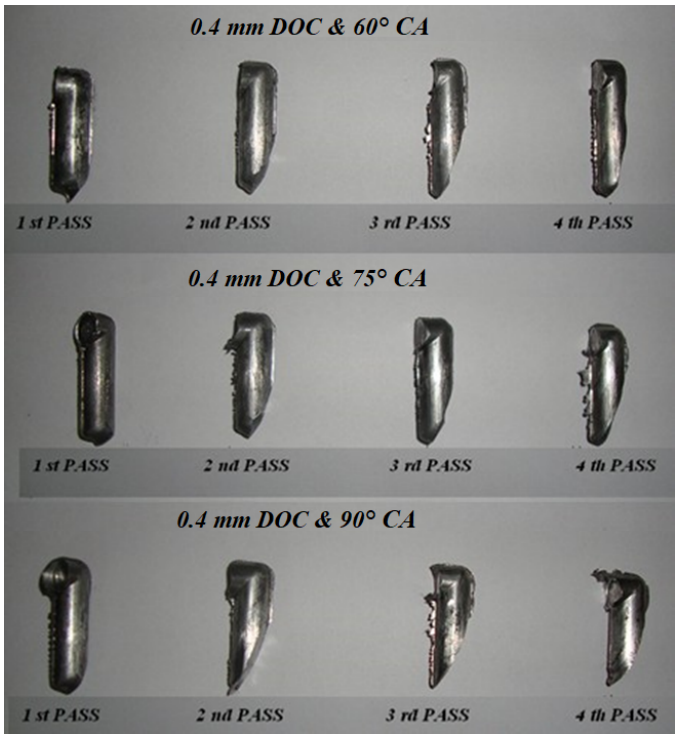

Fig. 7. Extruded ECAP samples, 0.4 mm DOC for 60°, 75° and 90°CA's

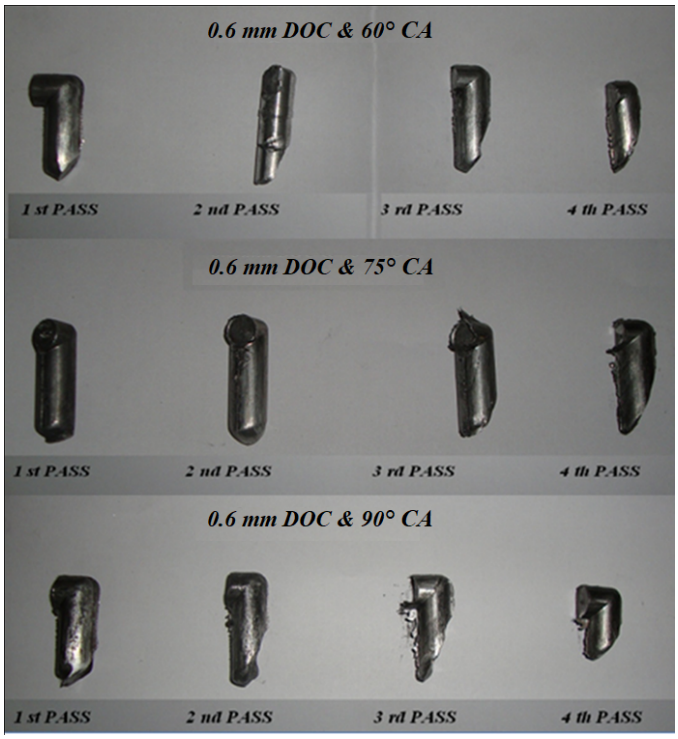

Fig. 8. Extruded ECAP samples, 0.6 mm DOC for 60°, 75° and 90°CA's

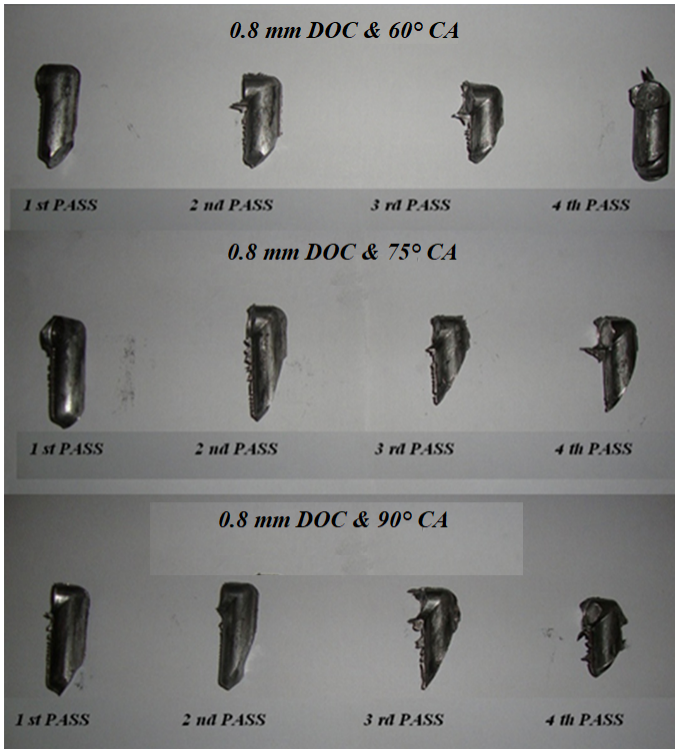

Fig. 9. Extruded ECAP samples, 0.8 mm DOC for 60°, 75° and 90°CA's

Although other cutting parameters may also play a role the DOC and CA was selected based on other investigations in the literature and due to their effect on both the width and thickness of the chips which may be significant for chip consolidation. The channel angle φ and corner angle ψ are kept constant at φ = 90° and ψ = 20°. The variation of the three input parameters were selected based on trail experimental runs that required that the extruded ECAP sample should not have major cracks or other significant defects. The variation levels of the input parameters eventually selected are presented in Table 1.

TABLE 1

Machining and ECAP Parameters with their limits

Parameters	Units	Notations	Levels		
			–1	0	1
Cutting edge angle (CA)	Degrees	A	60	75	90
Depth of Cut (DOC)	mm	B	0.4	0.6	0.8
Number of passes	—	C	2	3	4

3.2. Developing experimental design

Table 2 presents the selected design matrix. It comprises of a $2^3 = 8$ full factorial point, 6 centre points and 6-star points design which equates to 20 experimental runs. All input parameters at the intermediate level (0) constitute the centre points and the combinations of each of the process variables at either their minimum (–1) level or maximum (+1) level with the other two variables at the intermediate levels relating to the star points.

TABLE2

Experimental design matrix detailing the relative density and hardness comparisons between the experimental and predicted values

Trail No	ECAP process parameter			Relative Density		Hardness, HV	
	A (CA)	B (DOC)	C No. of Passes	Experimental value	Predicted value	Experimental value	Predicted value
1	–1	–1	–1	71.41	71.89	53.02	53.58
2	1	–1	–1	77.3	77.43	58.27	59.02
3	–1	1	–1	79.14	78.79	61.01	60.60
4	1	1	–1	90.31	89.89	72.11	71.56
5	–1	–1	1	82.05	82.47	64.10	64.26
6	1	–1	1	79.17	79.49	61.47	61.22
7	–1	1	1	91.09	90.93	73.01	72.80
8	1	1	1	94.01	93.51	76.01	75.28
9	–1	0	0	69.03	84.49	51.10	50.82
10	1	0	0	75.37	88.55	57.01	57.47
11	0	–1	0	81.41	87.35	63.13	62.25
12	0	1	0	97.31	97.81	79.11	79.96
13	0	0	–1	83.44	89.08	65.45	65.06
14	0	0	1	95.52	96.18	77.58	77.16
15	0	0	0	94.48	94.34	76.01	75.99
16	0	0	0	93.04	94.34	75.15	75.99
17	0	0	0	94.41	94.34	76.45	75.99
18	0	0	0	94.56	94.34	76.43	75.99
19	0	0	0	94.42	94.34	76.47	75.99
20	0	0	0	95.13	94.34	76.50	75.99

3.3. Development of empirical model

A second order polynomial regression model that includes the effects of the input parameters was developed linking the input parameters with the response outputs. Relative density and hardness are then a function of CA, DOC and the number of passes:

$$Y = F(A, B, C) \quad (1)$$

Where

Y – The response (Relative density and Hardness),
A – Edge cutting angle, Degrees,
B – Depth of cut, mm,
C – Number of pass.

For the three factors, the selected polynomial is expressed as

$$Y = b_0 + b_1A + b_2B + b_3C + b_{11}A^2 + b_{22}B^2 + + b_{33}C^2 + b_{12}AB + b_{13}AC + b_{23}BC \quad (2)$$

Where b_0 is the free term of the regression equation, the coefficients b_1, b_2, and b_3 are linear terms, the coefficients b_{11}, b_{22}, and b_{33}, are quadratic terms, and the coefficients, b_{12}, b_{13}, and b_{23}, are interaction terms. The values of the coefficients for the polynomial are calculated by regression analysis with the help of Design Expert 8.0.7.1.

4. Results

The final numerical models as obtained from this process is then:

$$\text{Relative density} = 94.34 + 2.03A + 5.23B + 3.55C + \\ + 1.39AB - 2.13\,AC + 0.39BC - 7.82A^2 - 1.76B^2 - 1.71C^2$$

$$\text{Hardness, HV} = 75.99 + 1.98A + 5.27B + 3.60C \\ + 1.38\,AB - 2.12\,AC + 0.38BC - 7.74A^2 - 1.73B^2 - 1.73C^2$$

The performance of the mathematical models for both relative density and hardness are evaluated by ANOVA and tabulated in Table 3 and Table 4 respectiely. The model F values of 343.03 and 335.39, for relative density and hardness respectively implies the model is significant. There is only a 0.01% chance that a model F-Value this large could occur due to noise.

Values of Prob > F less than 0.05 indicate model terms are significant. In this case A, B, C, AB, AC, A2, B2, C2 are significant model terms. Values greater than 0.10 indicate the model terms are not significant. The lack of fit F-value for relative density of 1.11 and hardness of 1.57 implies the lack of fit is not significant relative to the pure error. There is a 45.51% and 31.72% chance that a Lack of Fit F-value this large could occur due to noise for relative density and hardness respectievely. Non-significant lack of fit is good [27-30]. The Predicted R^2 values are in reasonable agreement with the Adjusted R^2 values.

TABLE 3

ANOVA analysis of relative density

Source	Sum of Squares	Degrees of freedom	Mean Square	F Value	p-value Prob > F	Significance
Model	1560.39	9	173.3771	343.0338	<0.0001	Yes
A-CA	56.44	1	56.4376	111.6641	<0.0001	—
B-DOC	372.88	1	372.8766	737.7519	<0.0001	—
C-Number of passes	172.07	1	172.0695	340.4467	<0.0001	—
AB	15.35	1	15.3458	30.3623	0.0003	—
AC	36.21	1	36.21005	71.64309	<0.0001	—
BC	1.23	1	1.23245	2.438453	0.1495	—
A^2	881.75	1	881.7473	1744.574	<0.0001	—
B^2	44.39	1	44.39092	87.82927	<0.0001	—
C^2	42.27	1	42.27068	83.6343	<0.0001	—
Residual	5.05	10	0.505423			—
Lack of Fit	2.66	5	0.532166	1.111736	0.4551	No
Pure Error	2.39	5	0.47868			—
Core Total	1565.45	19				—
R-Squared	0.99					
Adjusted R-Squared	0.99					
Predicted R-Squared	0.98					
Adequate Precision	58.41					

TABLE 4

ANOVA analysis of hardness

Source	Sum of Squares	Degrees of freedom	Mean Square	F Value	p-value Prob > F	Significance
Model	1549.42	9	172.16	335.39	<0.0001	Yes
A-CA	53.74	1	53.74	104.69	<0.0001	—
B-DOC	378.63	1	378.63	737.63	<0.0001	—
C-Number of passes	177.11	1	177.11	345.05	<0.0001	—
AB	15.13	1	15.13	29.47	0.0003	—
AC	36.12	1	36.12	70.38	<0.0001	—
BC	1.13	1	1.13	2.19	0.1696	—
A^2	862.98	1	862.98	1681.23	<0.0001	—
B^2	43.03	1	43.03	83.83	<0.0001	—
C^2	43.03	1	43.03	83.83	<0.0001	—
Residual	5.13	10	0.51			—
Lack of Fit	3.13	5	0.63	1.57	0.3172	No
Pure Error	2	5	0.4			—
Core Total	1554.55	19				—
R-Squared	0.99					
Adjusted R-Squared	0.99					
Predicted R-Squared	0.98					
Adequate Precision	57.62					

The Adequate Precision measures the signal to noise ratio. A ratio greater than 4 is desirable. There is an adequate signal in both models. Therefore these models can be used to navigate the design space. The normal probability graph of relative density and hardness shown in Fig. 10 which indicates that the residuals follow a straight line and this trend shows that there is a normal spread of errors for both models. Fig. 11 indicates that the random scatter pattern of residuals which denotes that, the proposed models are adequate and there is no violation of independent or constant variable. Fig.12 displays the predicted values versus experimental values of scattered responses and is close to the 45-degree line indicating that the predicted values and experimental values agreed with each other [31]. The influence of all parameters on the relative density and hardness of ECAP processed samples are represented by perturbation plots illustrated in Fig. 13. This graph indicates the change of output i.e response. When each input parameter moves away from reference point while the other parameters maintained with constant reference value.

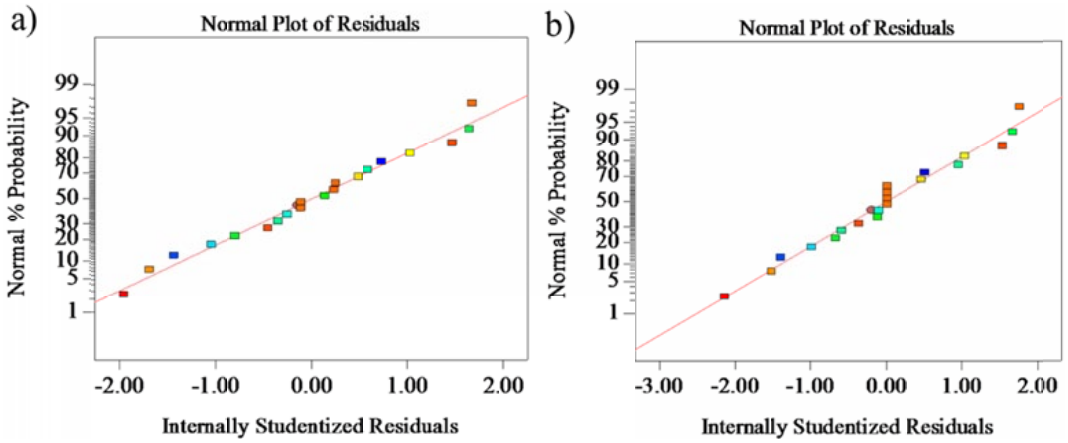

Fig. 10. Normal probability plot of residuals: a) Relative density, b) Hardness

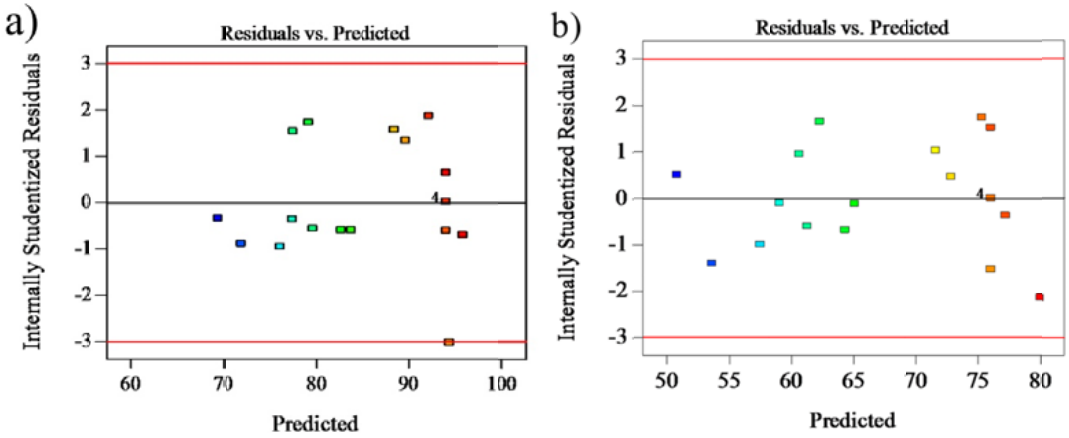

Fig. 11. Residual values versus predicted values: a) Relative density, b) Hardness

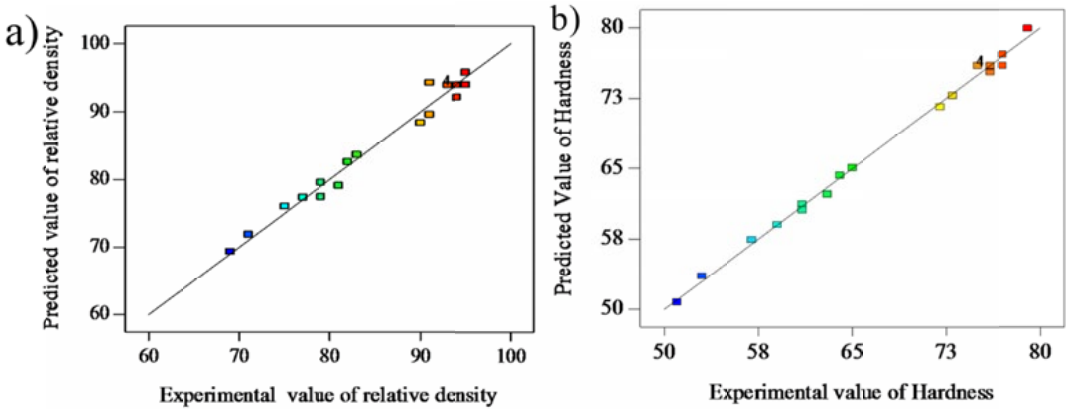

Fig. 12. Predicted values versus experimental values: a) Relative density, b) Hardness

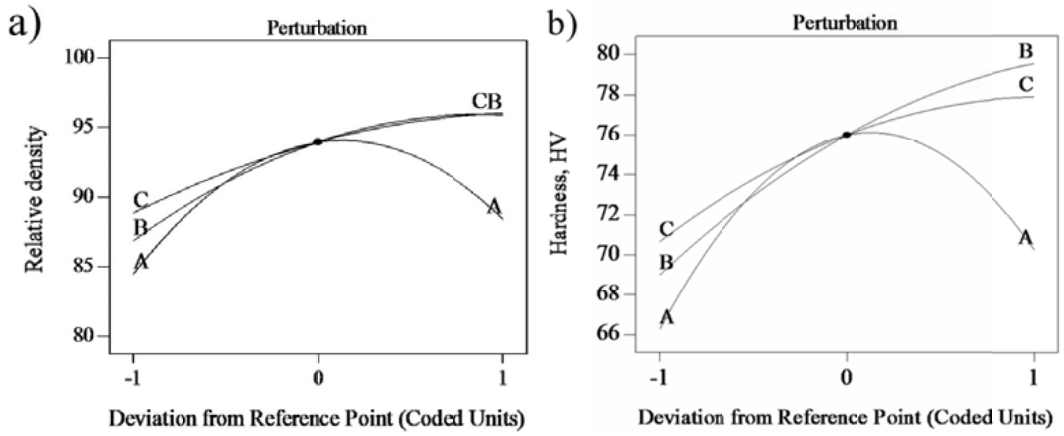

Fig. 13. Influence of all parameters on relative density and hardness (Perturbation plot)

5. Discussion

5.1. Effect of CA, DOC and Number of pass on microstructure

Extruded samples of the different parameter sets are shown in Fig. 7-9. The length of the specimen typically relates to the effectiveness of the consolidation albeit not exactly due to the differences in final shape. Longer means less consolidation whereas shorter implies better consolidation and higher relative density. The reduction in length due to the improved consolidation after successive passes are clearly visible. When the machined chips are consolidated by ECAP, the quality of the consolidated product is decided by its density and microstructure as reported by Misiolek et al. [32].

Optical micrographs and SEM surface morphology of the consolidated specimen after the 4th pass for the various process conditions are presented in Fig. 14(a-i) and Fig. 15(a-i). Chip

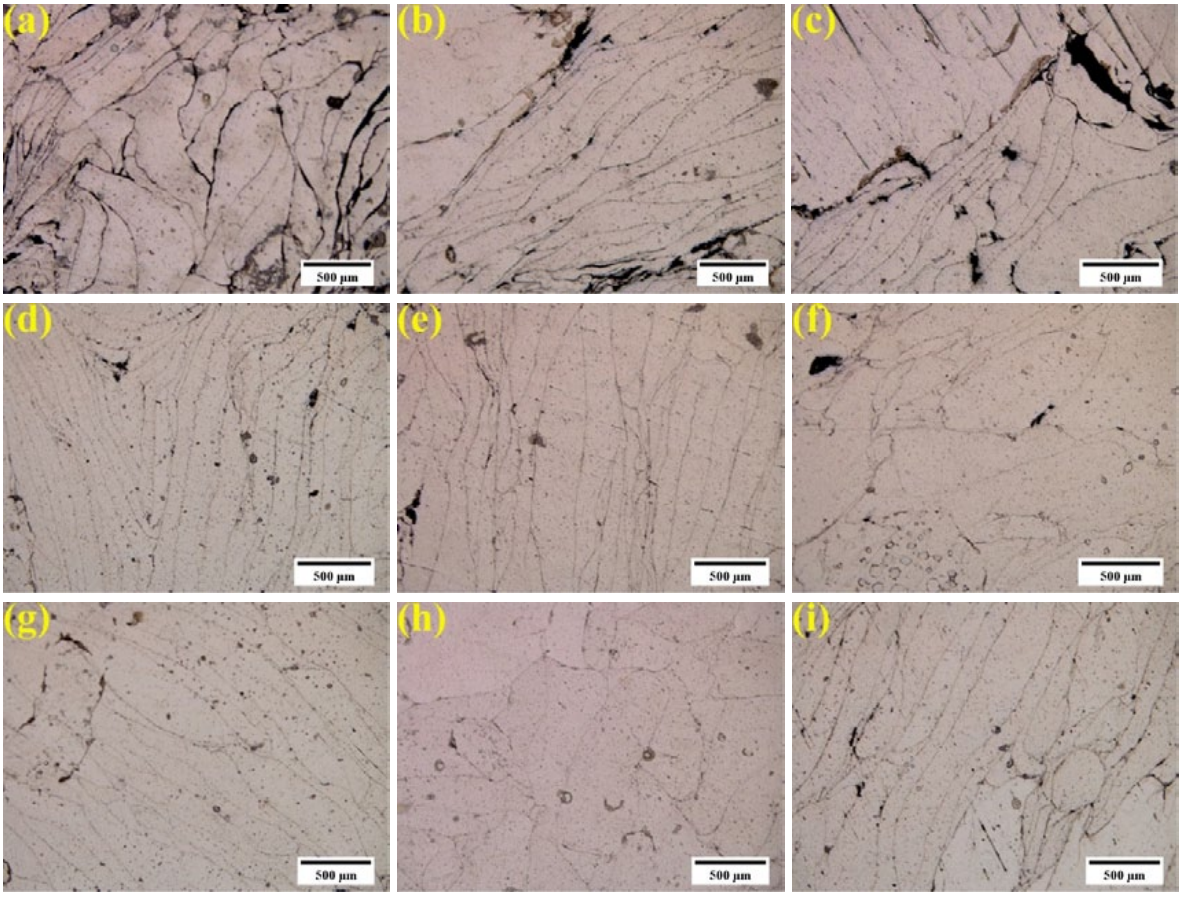

Fig. 14. Optical microstructure of consolidated chips for: (a) 0.4 mm DOC & 60°CA, (b) 0.4 mm DOC & 75°CA, (c) 0.4 mm DOC & 90°CA, (d) 0.6 mm DOC & 60°CA, (e) 0.6 mm DOC & 75°CA, (f) 0.6 mm DOC & 90°CA, (g) 0.8 mm DOC & 60°CA, (h) 0.8 mm DOC & 75°CA, (i) 0.8 mm DOC & 90°CA

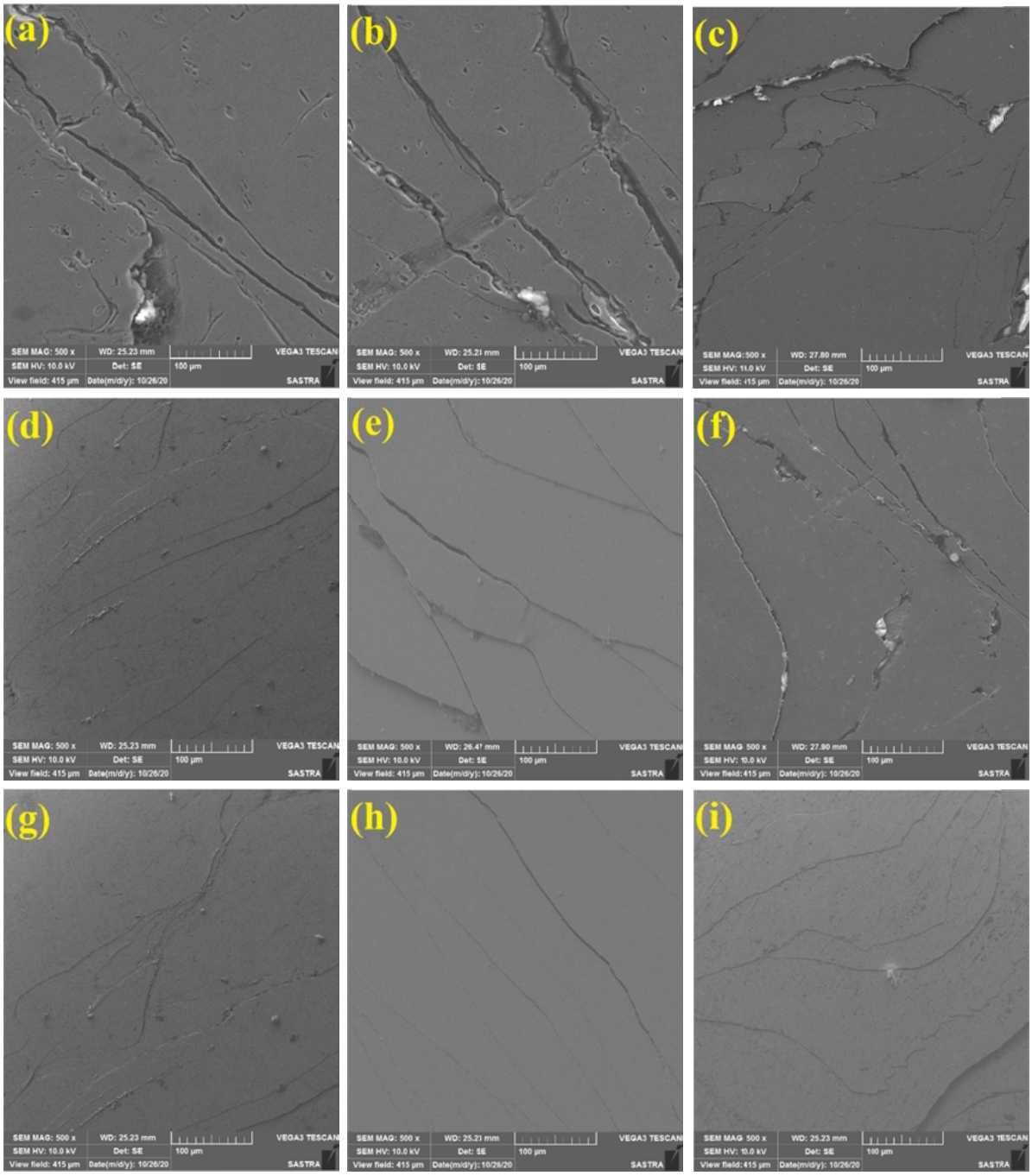

Fig. 15. Surface morphology of consolidated chips obtained by SEM for: (a) 0.4 mm DOC & 60°CA, (b) 0.4 mm DOC & 75°CA, (c) 0.4 mm DOC & 90°CA, (d) 0.6 mm DOC & 60°CA, (e) 0.6 mm DOC & 75°CA, (f) 0.6 mm DOC & 90°CA, (g) 0.8 mm DOC & 60°CA, (h) 0.8 mm DOC & 75°CA, (i) 0.8 mm DOC & 90°CA

interfaces are clearly visible for the micrographs associated with the lower DOC (0.4 mm, Fig. 14(a-c)). This improves slightly with less interfaces visible for the 0.6 mm DOC (Fig. 14(d-f)). A largely chip interface free and void less microstructure is visible for the 0.8 mm DOC (Fig. 14(g-i)) corresponding to the highest demonstrated consolidation and hardness. It should also be noted from Fig. 14(a-i) that, even though the number of passes is all similar (four) the chip interfaces are clearly visible in the cases of both the 0.4 and 0.6 mm DOC. This shows that the DOC and CA is more significant when compared to the number of passes for chip consolidation for these conditions.

5.2. Effect of CA, DOC and Number of pass on relative density

The effect of CA and DOC on relative density is shown in Fig. 16(a-b). The effect of CA on the concerned the relative density displays a bell-shaped curve which implies that the maximum relative density is achieved at an intermediate CA value of approximately 75°. The maximum relative density (best chip consolidation) of 97% is achieved for a 0.8 mm DOC and 75°CA. A smaller CA implies a thinner but wider chip and subsequently an increased chip surface area. This implies additional

surface strain energy and subsequently a larger consolidation area between chips that needs to be overcome if full consolidation is to be achieved. Furthermore, as the chip surface area increases, the formation of oxide layer also increases. The oxide layer is directly related with the size of the machined Al chip [33]. Hence, during the ECAP process an adequate amount of oxide layer has to be broken down before the bonding of chip interface for the chips with larger surface area, in the case of smaller CA. This resulted to insufficient consolidation as observed in the SEM images (refer to Fig. 15(a, d, g). In agreement with the above statement, Peng et al. [34] justified better consolidation in the solid-state recycling of machined chips when the surface area of the chip is more due to higher influence of oxide layer.

In the present study, a high CA implies the smallest chip surface area but does imply thicker chips that may require additional mechanical loading to deform and fully consolidate. An intermediate CA seems to balance these two effects and results in the best relative density. Besides, serrated and curled chips were produced during turning operation with the intermediate CA. This kind of chips have the tendency to turn into granules and powders during the ECAP process and occupy the voids between chip interfaces [35]. This is also one of the possible reasons for the better consolidation of chips with intermediate CA (refer to Fig. 15(b, e, h). The lowest relative density achieved is 71% for a 0.4 mm DOC and 60°CA. This parameter set displayed poor consolidation of chips due to the low CA effects alluded to above.

As far as DOC is concerned, in general the relative density is highest for the highest DOC and lowest at lower DOC. The effect is however relatively mild when compared to for example the chip angle. This is due to that fact that a high DOC implies wider chips with essentially the same thickness. This does however imply an increased surface area that need to be consolidate similar to the effect mentioned above for CA with one important difference in that the chip cross-sectional surface area effectively increases whereas with a change in CA it remains constant. This implies that effectively less chips are required for full consolidation due to their large cross-sectional area that effectively probably negates the effect of a larger consolidation surface area. The larger chips are effectively more likely to deform significantly during the initial passes of the ECAP process rather than just being displaced consolidation is mildly improved.

The effects of CA and the number of passes is presented in Fig. 17(a-b). It clearly shows that relative density increases progressively with each successive pass. Reports on ECAP chip consolidation showed improved hardness value on compacted chips than that of parent bulk material [19]. In this work a maximum relative density of 97% is achieved after the 4th pass at the optimum 75°CA.

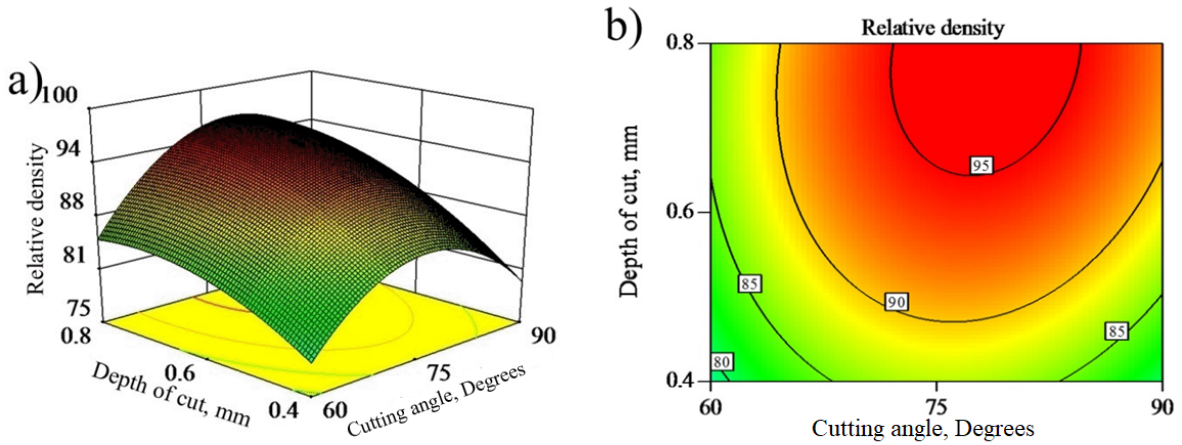

Fig. 16. Surface and contour plots representing the effect of DOC and CA on relative density

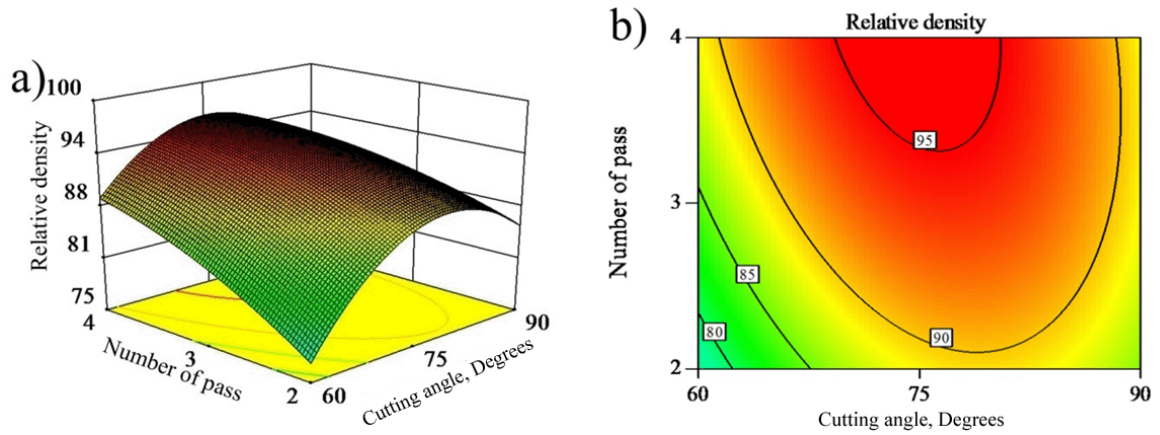

Fig. 17. Surface and contour plots representing the effect of number of passes and CA on relative density

5.3. Effect of CA, DOC and Number of pass on hardness

The effect of DOC and CA on the hardness as well as the effect of number of pass and CS on hardness are shown as surface and contour plots in Fig. 18(a-b) and Fig. 19(a-b), respectively. A very similar trend as outlined above for relative density is demonstrated for the hardness. A maximum hardness of 80 Hv is attained for a DOC of 0.8 mm and a 75°CA. Once again, the maximum hardness is attained at the maximum depth of cut and an intermediate value of the cutting angle. High and low cutting angles have a negative effect on hardness. It follows then that the hardness is essentially a nearly proportional function of the relative density and the hardness therefore varies for the same reasons as described above for the relative density. The hardness therefore also varies in a similar manner as a function of the number of passes. The best hardness of 80HV is achieved after the 4th pass at a DOC of 0.8 mm at the optimum 75°CA.

The main aim of the consolidation of machined chips is to produce a bulk CP Al product with refined grain structure by utilizing ECAP. The mechanism of chip consolidation in Al and its alloys follows two ways [34]: Firstly, the turned chips will develop oxide layer which hinders the consolidation and under the shear deformation during ECAP process, the layer will break. This leads to contact between chip surfaces and interface bonding of chips are attained. This kind of consolidation that takes place in ambient temperature conditions will develop physical consolidation of chips. As the shear stress developed will not be sufficient enough to break complete oxide layers, some micro cracks and voids are observed on the surfaces of the consolidated product as reported in the work of Güley et al. [36]. This is in line with the present study, where the microstructure of the consolidated chips showed clear chip interfaces and micro void in most of the conditions (refer to Fig. 14). In the present study due to the availability of micro voids, a full dense compact could not be attained (refer to table 2). Secondly, if the chip consolidation is conducted at elevated temperatures under severe plastic deformation, atomic diffusion bonding (metallurgical bonding) takes place as the chip interfaces are dissolved. A fully dense compact with no micro voids between chips are achieved due to plastic flow of metal that occurs during high temperature SPDs [37]. Furthermore, post heat treatment is suggested by McDonald et al. [38] where the chips consolidated by ECAP is subjected post heat treatment at elevated temperature can result in fully dense compact.

The present process may be further enhanced by conducting ECAP at elevated temperatures. An improvement in both relative density and hardness may be subsequently realized at elevated

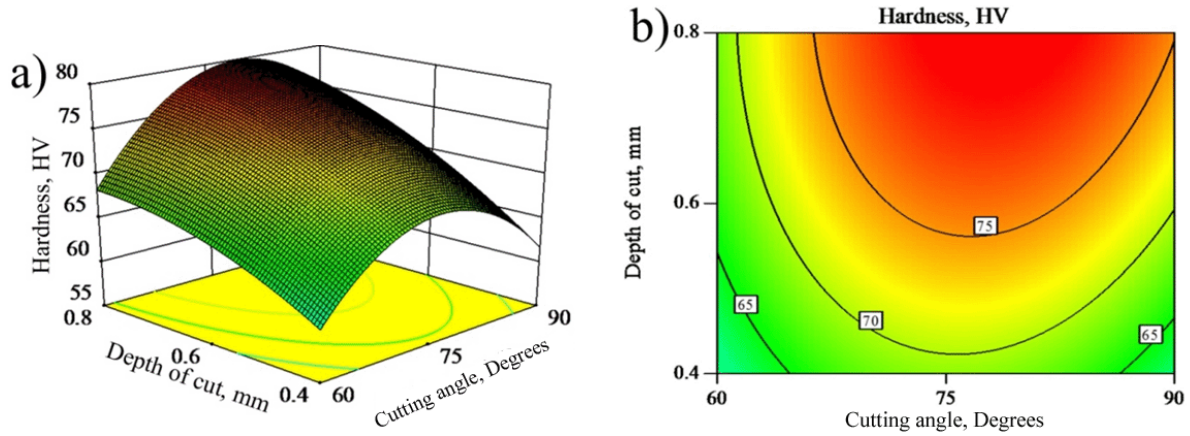

Fig. 18. Surface and contour plots representing the effect of DOC and CA on hardness

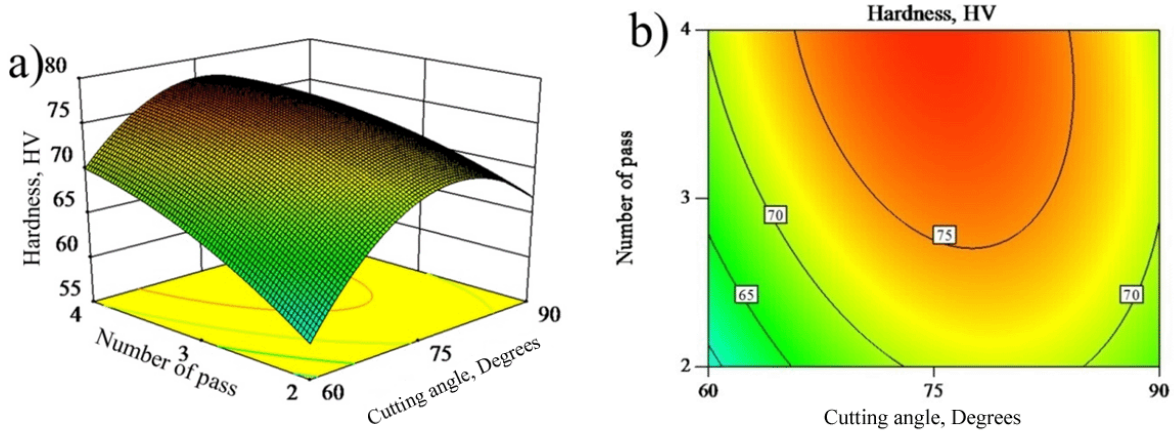

Fig. 19. Surface and contour plots representing the interaction effect on number of passes and CA on hardness

temperatures. The chip interface behaviour may also be improved due to defect diffusion across the interface. The mechanism of granulated chips is well documented in the work of Ravishankar et al. [39]. Higher temperatures may eventually help to achieve a 100% relative density bulk fine grained commercially pure Al with optimum hardness.

6. Conclusions

The following conclusions are drawn from this work:

- The relationships between process parameters for ECAP of CP Al have been established using response surface methodology. These were evaluated for accuracy with an ANOVA and scatter diagrams, and found to be satisfactory.
- Response graphs and contour plots were subsequently presented to demonstrate the effect of depth of cut, cutting angle and number of passes on the relative density and hardness of ECAP CP Al.
- The maximum relative density obtained is 97% for chips prepared with a 0.8 mm depth of cut, a 75° cutting angle and after 4 passes. This corresponded directly to the best hardness achieved of ~ 80HV.
- The hardness is essentially proportional to the relative density achieved. The maximum and minimum values of hardness corresponds directly the maximum and minimum values for the relative density.

Acknowledgements

One of the authors (Dr. P. Venkatachalam) sincerely thanks the Department of Science and Technology, New Delhi for the financial support through Fast track programme for young scientist. He also thanks the National Institute of Technology, Tiruchirappalli for providing technical support. One of the authors S.V would like to thank Mr. P. Rajesh of Jayaram College of Engineering & Technology, Tiruchirappalli for his extensive support during the experimental process.

REFERENCES

[1] G. Gaustad, E. Olivetti, R. Kirchain, Resources Conservation and Recycling **58**, 79-87 (2012). DOI: https://doi.org/10.1016/j.resconrec.2011.10.010

[2] Y.M. Shao, Resources Conservation and Recycling **117**, 25-33 (2017). DOI: https://doi.org/10.1016/j.resconrec.2015.09.015

[3] B. Wana, W. Chena, T. Lua, F. Liua, Z. Jianga, M. Maoa, Review of solid state recycling of aluminum chips, Resources Conservation and Recycling **125**, 37-47 (2017). DOI: http://dx.doi.org/10.1016/j.resconrec.2017.06.004

[4] Y. Ramu, P. Venkatachalam, S. Ramesh Kumar, B. Ravisankar, K. Jayasankar, P.S. Mukherjee, Transactions of the Indian Institute of Metals **63**, 813-817 (2010). DOI: https://doi.org/10.1007/s12666-010-0124-8

[5] M.I.A.E. Aal, E.Y. Yoon, H.S. Kim, Materials Science and Engineering A **560**, 121-128 (2013). DOI: https://doi.org/10.1016/j.msea.2012.09.045

[6] W. Tang, A.P. Reynolds, Journal of Materials Processing Technology **210**, 2231-2237 (2010). DOI: https://doi.org/10.1016/j.jmatprotec.2010.08.010

[7] J.R. Cui, W. Guo, H.J. Roven, Q.D. Wang, Y.J. Chen, T. Peng, Materials Science. Forum **667-669**, 1177-1182 (2011). DOI: https://doi.org/10.4028/www.scientific.net/MSF.667-669.1177

[8] M.A. Afifi, P.H.R. Pereira, Y.C. Wang, Y. Wang, S. Li, T.G. Langdon, Materials Science and Engineering A **684**, 617-625 (2017). DOI: https://doi.org/10.1016/j.msea.2016.12.099

[9] T.G. Langdon, Materials Science and Engineering A **462** (1-2), 3-11 (2007). DOI: https://doi.org/10.1016/j.msea.2006.02.473

[10] K. Xia, X. Wu, Scripta Materialia **53**, 1225-1229 (2005). DOI: https://doi.org/10.1016/j.scriptamat.2005.08.012

[11] M. H. Shaeri, M.T. Salehi, S.H. Seyyedein, M.R. Abutalebi, J.K. Park, Materials and Design. **57**, 250-257 (2014). DOI: https://doi.org/10.1016/j.matdes.2014.01.008

[12] Z.C. Duan, N.Q. Chinh, C. Xu, T.G. Langdon, Metallurgical and Materials Transactions A **41**, 802-809 (2010). DOI: https://doi.org/10.1007/s11661-009-0020-1

[13] R. D. Haghighi, S. Jahromi, A. Moresedgh, M.T. Khorshid. Journal of Materials Engineering and Performance **21**, 1885-1892 (2012). DOI: https://doi.org/10.1007/s11665-011-0108-9

[14] T. Ying, M.Y. Zheng, X.S. Hu, K. Wu, Transactions of Nonferrous Metals Society of China **20** (2), 604-607 (2010). DOI: https://doi.org/10.1016/S1003-6326(10)60547-X

[15] A.P. Zhilyaev, A.A. Gimazov, G.I. Raab, T.G. Langdon, Materials Science and Engineering A **486** (1-2),123-126 (2008). DOI: https://doi.org/10.1016/j.msea.2007.08.070

[16] P. Luo, D.T. McDonald, S. Palanisamy, M.S. Dargusch, K. Xia, Journal of Materials Processing Technology **213**, 469-476 (2013). DOI: https://doi.org/10.1016/j.jmatprotec.2012.10.016

[17] K.S. Ghosh, N. Gao, M.J. Starink, Materials Science and Engineering A **552**, 164-171 (2012). DOI: https://doi.org/10.1016/j.msea.2012.05.026

[18] M.V. Ali, K. Taheri, S.I. Hong, H.S. Kim, Materials Science and Engineering A **31** (9) 4076-4082 (2010). DOI: https://doi.org/10.1016/j.matdes.2010.04.056

[19] Y. Uluca, B.C. Rao, M. Ravishankar, T.L. Brown, J.B. Mann, S. Chandrasekar, W.D. Compton, Journal of SAE International 01, 01-07 (2005). DOI: https://doi.org/10.4271/2005-01-3306

[20] R.R.K.R. Vittel Rao, K. Gudimetla, M. Senthil Kumar, S. Ramesh Kumar, P. Venkatachalam, Materials Science Forum **969**, 361-366 (2019). DOI: https://doi.org/10.4028/www.scientific.net/MSF.969.361

[21] R.N. Chari, A. Kami, B.M. Dariani, Proceedings of the Institution of Mechanical Engineers, Part B: Journal of Engineering Manufacture 1-13 (2014). DOI: https://doi.org/10.1177/0954405414542855

[22] B. Saleh, J. Jiang, Q. Xu, R. Fathi, A. Ma, Y. Li, L. Wang, Metals and Materials International, (2020). DOI: https://doi.org/10.1007/s12540-020-00624-w

[23] S. Shahraki, I. Alinaghian, M. Motahari-Nezhad, Transactions of the Indian Institute of Metals **71** (3), 545-554 (2018). DOI: https://doi.org/10.1007/s12666-017-1187-6

[24] Z. Yang, K. Wang, Y. Yang, International Journal of Minerals, Metallurgy and Materials **27** (6), 792-800 (2020). DOI: https://doi.org/10.1007/s12613-019-1895-5

[25] K. Velmanirajan, A.S.A. Thaheer, R. Narayanasamy, C.A. Basha, Materials and Design **41**, 239-254 (2012). DOI: https://doi.org/10.1016/j.matdes.2012.05.027

[26] S.C. Vettivel, N. Selvakumar, R. Narayanasamy, N. Leema, Materials and Design **50**, 977-96 (2013). DOI: https://doi.org/10.1016/j.matdes.2013.03.072

[27] T. Udayakumar, K. Raja, T.M. Afsal Husain, P. Sathiya, Materials and Design **53**, 226-235 (2014). DOI: https://doi.org/10.1016/j.matdes.2013.07.002

[28] J.S. Kwak, International Journal of Machine Tool Manufacture **45** (3), 327-334 (2005). DOI: https://doi.org/10.1016/j.ijmachtools.2004.08.007

[29] S. Rajakumar, C. Muralidharan, V. Balasubramanian, Materials and Design **32** (5), 2878-2890 (2011). DOI: https://doi.org/10.1016/j.matdes.2010.12.025

[30] R. Palanivel, P. Koshy Mathews, N. Murugan, Journal of Central South university **20** (11), 2929-2938 (2013). DOI: https://doi.org/10.1007/s11771-013-1815-1

[31] A. Heidarzadeh, T. Saeid, Materials and Design **52**, 1077-1087 (2013). DOI: https://doi.org/10.1016/j.matdes.2013.06.068

[32] W.Z. Misiolek, M. Haase, N.B. Khalifa, A.E. Tekkaya, M. Kleiner, CIRP Annals Manufacturing Technology **61**, 239-242 (2012). DOI: https://doi.org/10.1016/j.cirp.2012.03.113

[33] M.L. Hu, Z.S. Ji, X.Y. Chen, Z.K. Zhang, Z.K., Materials Characterization **59**, 385-389 (2008). DOI: https://doi.org/10.1016/j.matchar.2007.02.002

[34] T. Peng, Q.D. Wang, Y.K. Han, J. Zheng, W. Guo, Journal of Alloys and Compounds **503**, 253-259 (2010). DOI: https://doi.org/10.1016/j.jallcom.2010.05.011

[35] A.R. Anilchandra, M.K. Surappa, Journal of Materials Processing Technology **210**, 423-428 (2010). DOI: https://doi.org/10.1016/j.jmatprotec.2009.10.002

[36] V. Güley, A. Güzel, A. Jäger, N.B. Khalifa, A.E. Tekkaya, W.Z. Misiolek, Materials Science and Engineering A. 574, 163-175 (2013). DOI: https://doi.org/10.1016/j.msea.2013.03.010

[37] T. Ying, M.Y. Zheng, X.S. Hu, K. Wu, Transactions of Nonferrous Metals Society of China **22**, 2906-2912 (2010). DOI: https://doi.org/10.1016/S1003-6326(10)60547-X

[38] D.T. McDonald, P. Luo, S. Palanisamy, M.S. Dargusch, K. Xia, Key Engineering Materials **520**, 295-300 (2012). DOI: https://doi.org/10.4028/www.scientific.net/KEM.520.295

[39] M. Ravishankar, S. Chandrasekar, A.H. King, W.D. Compton, Acta Materialia **53** (18), 4781-4793 (2005). DOI: https://doi.org/10.1016/j.actamat.2005.07.006